Design and Evaluation of an Eight Channel TX/RX Hybrid Applicator for Imaging and Targeted RF-Heating at 7.0 T

Lukas Winter[1], Celal Özerdem[1], Werner Hoffmann[2], Helmar Waiczies[1], Davide Santoro[1], Alexander Müller[1], Tomasz Lindel[1], Wolfgang Renz[1,3], Conrad Martin[1], Frank Seifert[2], Bernd Ittermann[2], and Thoralf Niendorf[1,4]

[1]Berlin Ultrahigh Field Facility (B.U.F.F.), Max-Delbrueck-Center for Molecular Medicine, Berlin, Germany, [2]Physikalisch Technische Bundesanstalt (PTB), Berlin, Germany, [3]Siemens Healthcare, Erlangen, Germany, [4]Experimental and Clinical Research Center (ECRC), Charité - University Medicine Campus Berlin Buch, Berlin, Germany

Introduction: Recent reports demonstrate that radiative dipole antennas are beneficial for ultrahigh field (7.0T) imaging since they provide enhanced B1+ efficiency for deep lying regions and a nearly symmetrical B1+ field distribution[1]. Also, it has been shown that electric-dipole current components dominate the ultimate intrinsic signal to noise ratio (SNR) at ultrahigh fields [2]. Radiative elements are commonly used for radiofrequency (RF) hyperthermia induced targeted heating of biological tissue. This approach is used at lower fields as an adjunctive therapy for established cancer treatments including radiotherapy and chemotherapy [3-4]. Combining RF hyperthermia and MR imaging is conceptually appealing to pursue spatially and temporally controlled and monitored RF heating. Here, the traits of ultrahigh fields can be put to use including an improved baseline SNR for high spatial resolution MRI and RF technology driven by the move towards multi-transmit/receive (TX/RX) architecture. Since the RF spin-excitation frequency (297 MHz) exceeds that of conventional RF hyperthermia systems (<140MHz) RF hyperthermia at UHF holds the promise to further sharpen the focal width of local hotspots [5-6]. To this end, this study demonstrates the feasibility of an 8 channel TX/RX hybrid applicator tailored for imaging and targeted hyperthermia at 7.0 T.

Methods: An 8 channel TX/RX applicator for imaging and RF hyperthermia at 297MHz was designed and built (Fig. 1a). The applicator consists of eight bowtie antennas (size: 70x50mm) (Fig. 1b). Highly surge proof (12kV) matching and tuning trim capacitors were used to allow high power throughput during RF heating. To shorten the wavelength the antenna was immersed in a water solution (75x155x40mm, 0.7g MnCl/l). The evaluation of the design was performed using numerical field simulations with CST Microwave Studio (CST GmbH, Darmstadt Germany). Imaging parameters were derived from numerical SAR_{10g} simulations together with the voxelmodell Duke from the Virtual Family (ITIS Foundation, Zurich, Switzerland) according to IEC guidelines 60601-2-33 Ed.3. Two cylindrical phantoms (r_1=90mm, r_2=60mm, l=250mm, ε_1=75, σ_1=0.72 S/m, ε_2=71, σ_2=1.12 S/m) with polyethylen tubes insert were built for validation purposes [7]. B1+ maps were simulated and acquired using a pulse preparation method. Noise correlation between the elements was measured using a noise prescan. Transient temperature distributions were simulated and validated in phantom studies using the proton resonance frequency shift (PRFS) method together with optical thermo sensors (Lumasense Technologies, Santa Clara, USA) [8]. A 7.0 T whole body MRI system (Magnetom, Siemens, Erlangen, Germany) together with an 8x1kW RF amplifier (Stolberg HF Technik AG, Stolberg-Vicht, Germany) with variable phase and aplitude settings was used for imaging and heating.A gradient echo technique was used for imaging (1.2x1.2x6mm³, TE/TR = 12/60ms). For RF heating a rectangular pulse (170V) with a duty cycle of 10% was applied.

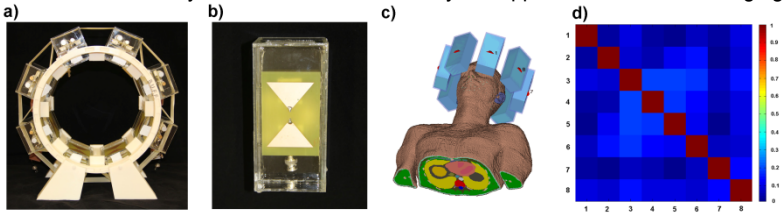

Fig. 1: Eight channel transmit receive applicator (a), a single element bow tie dipole antenna building block (b), the simulation setup (c) and the noise correlation matrix (d).

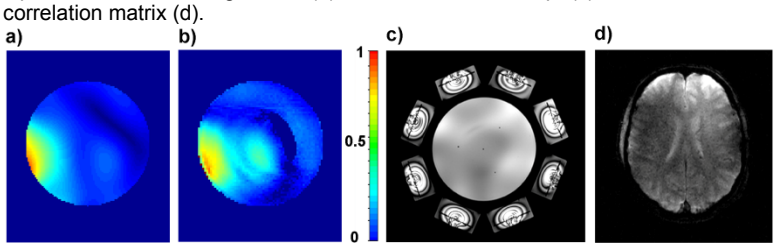

Fig. 2: Imaging performance of the hybrid applicator. Simulated (a) and measured (b) B1+ maps of one element and phantom (r_1). c) gradient echo image of the phantom d) Preliminary result from gradient echo imaging of a healthy brain.

Results: Matching and tuning parameters were below -27dB. Decoupling between elements was found to be below -21dB. Maximum measured noise correlation between elements was 0.2 (Fig. 1d). Simulated and measured B1+ maps, phantom images and preliminary *in vivo* results are depicted in Fig. 2. Numerical simulations showed higher SAR values in the center of the phantom versus surface regions (Fig. 3). These SAR hotspots could be modulated and steered successfully to other arbitrary positions and regions within the phantom as demonstrated in Fig. 3. For this purpose the amplitude and phase contributions of each individual bow tie antenna element were changed. The ISO SAR 90% hotspot has the dimensions of 18x18x26mm³. The temperature simulations show an increase in temperature of 9K in the center (5min. heating, 25W CW) compared to 6K at the surface. In the experimental setup, thermo optical probes showed a temperature increase of 5K in the center of the phantom.

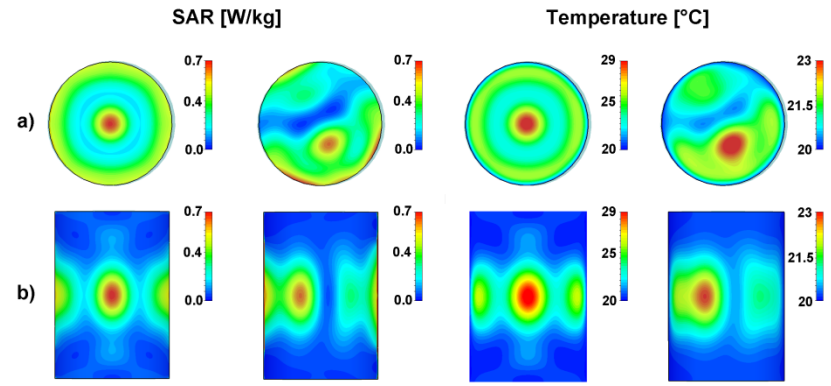

Fig. 3: Point SAR simulations and resulting temperature simulations (25W with different phase settings in an axial (a) and coronal (b) view of the phantom (radius=90mm). The diameter of the focal width of the SAR/temperature hot spots was found to be approximately 18 mm.

Discussion and Conclusions: The hybrid applicator showed encouraging results for imaging and RF heating. Targeted, focal deep seated SAR/temperature hotspots could be successfully generated. An increase in the number of elements could further enhance the RF modulation and steering abilities for targeted 3D RF heating. We anticipate to use heavy water to reduce power losses in the antenna and to prevent proton excitations at the antennas tip. To further cool the surface area a water bolus together with a cooling system will be integrated into the current approach. These improvements will help to further drive and explore the capabilities of the proposed hybrid applicator and its implications for dedicated MR applications including targeted cancer treatment - which goes beyond current liver and abdominal applications - plus targeted drug and MR contrast agent delivery.

References: [1] Raaijmakers, A., et al., MRM, 2011; [2] Lattanzi, R. and D.K. Sodickson, ISMRM Proc,2011; [3] Nadobny, J., et al., Med Phys, 2003; [4] Issels, R.D., et al., Lancet Oncol, 2010 [5] Dobšícek Trefná, H., et al., Int J Hyperther, 2010 [6] Yang, X., et al., ISMRM Proc, 2011; [7] Yang, Q.X., et al., MRM, 2004; [8] Wonneberger, U., et al., JMRI, 2010